Int. J. Electrochem. Sci., 9 **(2014)** 1415 - 1438

International Journal of
ELECTROCHEMICAL
SCIENCE
www.electrochemsci.org

Synthesis, Characterization and in vitro Biological Activity of Mixed Transition Metal Complexes of Lornoxicam with 1,10-phenanthroline

Walaa H. Mahmoud[1], *Gehad G. Mohamed*[1*], *Maher M.I. El-Dessouky*[1]

Chemistry Department, Faculty of Science, Cairo University, Giza, 12613 Egypt
[*]E-mail: ggenidy68@hotmail.com

Received: 14 October 2013 / *Accepted:* 17 November 2013 / *Published:* 5 January 2014

A new series of Cr(III), Mn(II), Fe(II), Fe(III), Co(II), Ni(II) and Zn(II) ternary complexes derived from lornoxicam and 1,10-phenanthroline (Phen) have been synthesized and characterized by spectroscopic studies. The coordination possibility of the two ligands towards metal ions have been proposed in the light of elemental analysis, spectral (mass, IR, UV–vis, ^{1}H NMR and ESR), X-ray powder diffraction, magnetic and thermal studies. IR spectra show that LOR and Phen are coordinated to the metal ions in a neutral bidentate manner. The molar conductance measurements of the complexes in DMF correspond to electrolytic nature of the ternary complexes, thus, these complexes may be formulated as $[M(LOR)(Phen)Cl_2]X_n.yH_2O$ (M = Cr(III) (n = 1, y = 2) and Ni(II) (n = 0, y = 1); $[M(LOR)(Phen)(H_2O)_2](BF4)_2$ (M = Fe(II), Co(II), Cu(II) and Zn(II)) and $[M(LOR)_2(Phen)]X_n.yH_2O$ (M = Mn(II) (n = y = 2) and Fe(III) (n = 3, y = 0)). On the basis of magnetic moment, electronic and ESR spectral studies, an octahedral geometry has been assigned for the ternary complexes. Furthermore, the kinetic and thermodynamic parameters for the different decomposition steps were calculated using the Coats–Redfern and Horowitz–Metzger methods. Also, the two ligands, in comparison to ternary metal complexes are screened for their antimicrobial and anticancer activity against breastic cancer cell line. The results showed that the metal complexes be more active than the parent LOR ligand but less active than 1,10-phenanthroline free ligand. The Co(II) and Cu(II) metal complexes completely missed anticancer activity.

Keywords: Lornoxicam; 1,10-phenanthroline, ternary metal complexes; spectroscopy; TG-DTG; antimicrobial and antitumor activity.

1. INTRODUCTION

Metal-based drugs are a research area of increasing interest for inorganic, pharmaceutical and medicinal chemistry and have concentrated much attention as an approach to new drug development [1]. As far as we know, the selection of appropriate metal ions and organic ligands is the key in the

construction of complexes. Metal ions, especially their radii and coordination geometry, determine the extending direction and coordination modes of the organic ligands, which is important for the structure of the complexes. Among the metal complexes, those of 1,10-phenanthroline have attracted line. 1,10-phenanthroline as chelating nitrogen donor ligands is among the most efficient chelators for transition and post-transition metal ions with which it form stable complexes in solution. The presence of aromatic and/or heteroaromatic groups into the structure of nitrogen donors gives these ligands with additional properties. For instance, poly nitrogen donors containing aromatic and/or heteroaromatic groups conjugate the ligational ability with the photophysical properties typical of these groups and, accordingly, they have been widely used as chemosensors for metal ions in solution, since their coordination may affect the properties of the photosensitive group giving rise to an optical response [2-4]. It is well known been also reported that some ternary complexes of 1,10-phenanthroline (phen) e.g. [Cu(phen)] have an antitumor activity where it inhibited DNA or RNA polymerase activities [4, 5].

Microbial infections often produce pain and inflammation. Chemotherapeutic, analgesic and anti-inflammatory drugs are prescribed simultaneously in normal practice. The compound possessing all three activities is not common. Anti-inflammatory, analgesic and antipyretic activities are known for some Pyridine and phenol derivatives [6-8]. These compounds are able to block cartilage destruction during the inflammatory process and thus are a promising class of anti-inflammatory compounds [9]. Lornoxicam drug (Fig.1) is a member of non steroidal anti-inflammatory drugs (NSAIDs) that characterized by rapid and complete uptake in the bloodstream and in turn, the presence of the metallic ions can affect bioavailability of the drug thus possessing a fast analgesic action [5].

Therefore, two aspects have been examined in the present work. First we synthesized and investigated the ternary complexes of LOR and 1,10-Phenanthroline with different transition metals by different spectral tools. Secondly, studying their in vitro antimicrobial and anticancer activity after complexation.

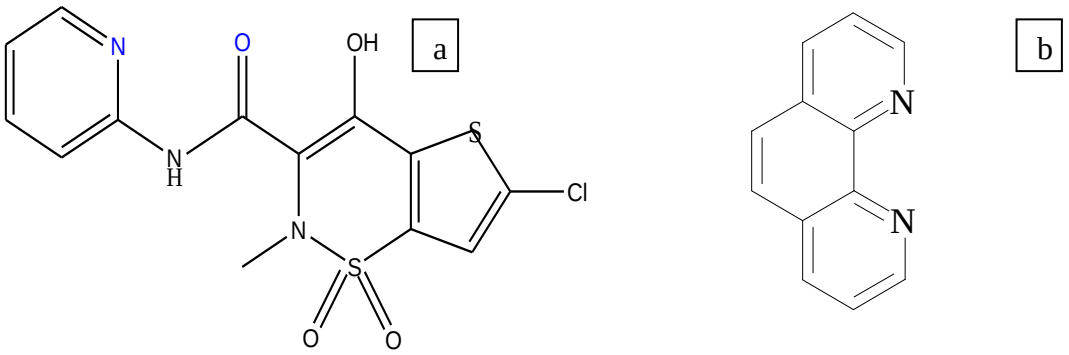

Figure 1. Structures of (a) lornoxicam and (b) 1,10-phenanthroline.

2. EXPERIMENTAL

2.1 Material and reagent

All chemicals used were of the analytical reagent grade (AR), and of highest purity available. The chemicals used included lornoxicam drug which was supplied from National Organization for

Drug Control and Research, 1,10-phenanthroline (Merck), $CrCl_3 \cdot 6H_2O$ and $MnCl_2 \cdot 2H_2O$ (Sigma), $NiCl_2 \cdot 6H_2O$ (BDH), $FeCl_3 \cdot 6H_2O$ (Prolabo), $Fe(BF_4)_2.6H_2O$ and $Co(BF_4)_2.6H_2O$ (Aldrich), $Cu(BF_4)_2.6H_2O$ (Merck) and $Zn(BF_4)_2$ (Strem Chemicals). Organic solvents were spectroscopic pure from BDH included ethanol, diethyl ether and dimethyl formamide. Hydrogen peroxide, sodium chloride, sodium carbonate and sodium hydroxide (A.R.) were used.

Human tumor cell lines (Brest cell) were obtained frozen in liquid nitrogen (-180 ^{0}C) from the American Type Culture Collection. The tumor cell lines were maintained in the National Cancer Institute, Cairo, Egypt, by serial sub-culturing.

2.2 Solutions

A fresh stock solution of $1x10^{-3}$ M of LOR (0.372 g/L) was prepared in the appropriate volume of absolute ethanol and DMF by a ratio (1:5 v/v ethanol:DMF). Dimethylsulphoxide (DMSO) (Sigma Chemical Co., St. Louis, Mo, and U.S.A): It was used in cryopreservation of cells. RPMI-1640 medium (Sigma Chemical Co., St. Louis, Mo, and U.S.A) was used. The medium was used for culturing and maintenance of the human tumor cell lines. The medium was supplied in a powder form. It was prepared as follows: 10.4 g medium was weighed, mixed with 2 g sodium bicarbonate, completed to 1 L with distilled water and shaked carefully till complete dissolution. The medium was then sterilized by filtration in a Millipore bacterial filter (0.22 μm). The prepared medium was kept in a refrigerator (4 ^{0}C) and checked at regular intervals for contamination. Before use the medium was warmed at 37 ^{0}C in a water bath and the supplemented with penicillin/streptomycin and FBS.

Sodium bicarbonate (Sigma Chemical Co., St. Louis, Mo, USA) was used for the preparation of RPMI-1640 medium. 0.05% isotonic Trypan blue solution (Sigma Chemical Co., St. Louis, Mo, USA) was prepared in normal saline and was used for viability counting. 10% Fetal Bovine Serum (FBS) (heat inactivated at 56 °C for 30 min), 100 units/ml Penicillin and 2 mg/ml Streptomycin were supplied from Sigma Chemical Co., St. Louis, Mo, USA and were used for the supplementation of RPMI-1640 medium prior to use. 0.025% (w/v) Trypsin (Sigma Chemical Co., St. Louis, Mo, USA) was used for the harvesting of cells. 1% (v/v) Acetic acid (Sigma Chemical Co., St. Louis, Mo, USA) was used for dissolving the unbound SRB dye. 0.4% Sulphorhodamine-B (SRB) (Sigma Chemical Co., St. Louis, Mo, USA) dissolved in 1 % acetic acid was used as a protein dye. A stock solution of trichloroacetic acid (TCA, 50%, Sigma Chemical Co., St. Louis, Mo, USA) was prepared and stored. 50 μl of the stock was added to 200 μl RPMI-1640 medium/well to yield a final concentration of 10 % used for protein precipitation. 100% Isopropanol and 70 % ethanol were used. Tris base 10 mM (pH 10.5) was used for SRB dye solubilization. 121.1 g of tris base was dissolved in 1000 ml of distilled water and pH was adjusted by HCl acid (2 M).

2.3. Measurements

Microanalyses of carbon, hydrogen and nitrogen were carried out at the Microanalytical Center, Cairo University, Egypt, using CHNS-932 (LECO) Vario Elemental Analyzer. Analyses of the

metals followed the dissolution of the solid complex in concentrated HNO_3, neutralizing the diluted aqueous solutions with ammonia and titrating the metal solutions with EDTA. FT-IR spectra were recorded on a Perkin-Elmer 1650 spectrometer (4000–400 cm^{-1}) in KBr pellets. Electronic spectra were recorded at room temperature on a Shimadzu 3101pc spectrophotometer as solutions in ethanol. ^1H NMR spectra, as a solution in DMSO-*d6*, were recorded on a 300 MHz Varian-Oxford Mercury at room temperature using TMS as an internal standard. Electron spin resonance spectra were also recorded on JES-FE2XG ESR spectrophotometer at Microanalytical Center, Tanta University.

Mass spectra were recorded by the EI technique at 70 eV using MS-5988 GS-MS Hewlett-Packard instrument at the Microanalytical Center, National Center for Research, Egypt. The molar magnetic susceptibility was measured on powdered samples using the Faraday method. The diamagnetic corrections were made by Pascal's constant and $Hg[Co(SCN)_4]$ was used as a calibrant Molar conductivities of 10^{-3} M solutions of the solid complexes in DMF were measured on the using Jenway 4010 conductivity meter. The thermogravimetric analyses (TG, DTG and DTA) of the solid complexes were carried out from room temperature to 800 °C using a Shimadzu TG-50H thermal analyzer. The X-ray powder diffraction analyses were carried out by using Philips Analytical X-Ray BV, diffractometer type PW 1840. Radiation was provided by copper target (Cu anode 2000 W) high intensity X-ray tube operated at 40KV and 25 mA. Divergence and the receiving slits were 1 and 0.2, respectively. The anticancer activity was performed at the National Cancer Institute, Cancer Biology Department, Pharmacology Department, Cairo University. The optical density (O.D.) of each well was measured spectrophotometrically at 564 nm with an ELIZA microplate reader (Meter tech. Σ 960, U.S.A.).

2.4. Preparation of mixed ligand complexes

The present mixed complexes were prepared by mixing equal amounts (0.01 mol) of hot saturated ethanolic solution of the first ligand (lornoxicam) and second ligand (1,10-phenanthroline) with the same ratio of metal chloride or borate salts. The mixture was refluxed for three hours. The resulting complexes were filtered and washed several times with hot ethanol until the filtrates become clear. The solid complexes then dried in desiccator over anhydrous calcium chloride. The yield ranged from 74-91%.

M(II) or M(III) + one or two moles of L^1 + L^2 $\longrightarrow$ $[ML^1L^2]^+$ or $[ML_2{}^1L^2]^+$

M(II) = Mn(II), Fe(II), Co(II), Ni(II), Cu(II), Zn(II), M(III) = Cr(III), Fe(III), L^1 = lornoxicam, L^2 = 1,10-phenanthroline.

The dried complexes were subjected to elemental and spectroscopic analyses. The obtained complexes are soluble in ethanol, DMF and DMSO. All melting points of the complexes were measured and found to be >200 °C.

2.5. Spectrophotometric studies

The absorption spectra of LOR and 1,10-phenanthroline free ligands and their mixed metal complexes under study were scanned within the wavelength range from 200 to 600 nm.

2.6. Antimicrobial Activity

A filter paper disk (5 mm) was transferred into 250 ml flasks containing 20 ml of working volume of tested solution (100 g/ml). All flasks were autoclaved for 20 min at 121 ◦C. LB agar media surfaces were inoculated with two investigated bacteria (gram positive and gram negative) and two strains of fungi then, transferred to a saturated disk with a tested solution in the center of Petri dish (agar plates). Finally, all these Petri dishes were incubated at 25 ◦C for 48 h where clear or inhibition zones were detected around each disk. Control flask of the experiment was designed to perform under the same condition described previously for each microorganism but with dimethylformamide solution only and by subtracting the diameter of inhibition zone resulting with dimethylformamide from that obtained in each case, so antibacterial activity could be calculated [10]. All experiments were performed as triplicate and data plotted were the mean value.

2.7. Anticancer activity:

Potential cytotoxicity of the compounds was tested using the method of Skehan et al [11]. Cells were plated in 96-multiwell plate (104 cells/well) for 24 h before treatment with the compounds to allow attachment of cell to the wall of the plate. Different concentrations of the compounds under investigation (0, 5, 12.5, 25, 50 and 100 μg/ml) were added to the cell monolayer triplicate wells were prepared for each individual dose. The monolayer cells were incubated with the compounds for 48 h at 37 °C and in 5% CO_2 atmosphere. After 48 h, cells were fixed, washed and stained with SRB stain. Excess stain was washed with acetic acid and attached stain was recovered with tris-EDTA buffer. The optical density (O.D.) of each well was measured spectrophotometrically at 564 nm with an ELIZA microplate reader and the mean background absorbance was automatically subtracted and mean values of each drug concentration was calculated. The relation between surviving fraction and drug concentration is plotted to get the survival curve of Breath tumor cell line for each compound.

Calculation:

The percentage of cell survival was calculated as follows:

Survival fraction = O.D. (treated cells)/ O.D. (control cells).

The IC_{50} values (the concentrations of LOR, Phen or metal complexes required to produce 50 % inhibition of cell growth). The experiment was repeated three times for MCF7 cell line.

3. RESULT AND DISCUSSION

3.1. Microanalysis

The elemental analysis data of the complexes (Table 1) show the formation of the complexes in the ratio of 1:1:1 for $[ML^1L^2]$ except for Mn(II) and Fe(III) complexes where the ratio is 1:2:1 corresponding to a metal–lornoxicam–1,10-phenanthrolin. It is found that the theoretical values are in agreement with the found values.

Table 1. Analytical and physical data of LOR ternary complexes with1,10-phenanthroline.

Compound (Molecular Formula)	Colour (%yield)	M.p. (°C)	% Found (Calcd.)					$\mu_{eff.}$ (B.M.)	Λ_m $\Omega^{-1}mol^{-1}$ cm^2
			C	H	N	S	M		
$[Cr(LOR)(Phen)Cl_2]Cl.2H_2O$ ($C_{25}H_{22}Cl_4CrN_5O_5S_2$)	Green (90)	230	40.76 (40.20)	2.76 (2.95)	9.66 (9.38)	8.86 (8.58)	6.85 (6.97)	4.87	80
$[Mn(LOR)_2(Phen)]Cl_2 \cdot 2H_2O$ ($C_{38}H_{32}Cl_4N_8O_{10}S_4Mn$)	Brown (83)	220	42.05 (42.00)	2.98 (2.95)	10.14 (10.32)	12.03 (11.79)	4.95 (5.07)	5.12	130
$[Fe(LOR)(Phen)(H_2O)_2](BF_4)_2$ ($C_{25}H_{22}B_2ClF_8FeN_5O_6S_2$)	Reddish Brown (87)	265	36.78 (36.67)	2.88 (2.69)	8.77 (8.56)	7.96 (7.82)	6.50 (6.85)	5.33	125
$[Fe(LOR)_2(Phen)]Cl_3$ ($C_{38}H_{28}Cl_5FeN_8O_8S_4$)	Dark Brown (91)	195	41.64 (41.98)	2.76 (2.58)	10.40 (10.31)	11.86 (11.78)	5.15 (5.16)	5.64	195
$[Co(LOR)(Phen)(H_2O)_2](BF_4)_2$ ($C_{25}H_{22}B_2ClCoF_8N_5O_6S_2$)	Dark Brown (86)	215	36.14 (36.59)	2.54 (2.68)	8.82 (8.54)	70.68 (7.80)	7.22 (7.13)	5.20	145
$[Ni(LOR)(Phen)Cl_2].H_2O$ ($C_{25}H_{20}Cl_3N_5NiO_5S_2$)	Green (89)	220	42.80 (42.92)	3.01 (2.86)	9.95 (10.01)	9.35 (9.16)	8.24 (8.44)	2.99	12
$[Cu(LOR)(Phen)(H_2O)_2](BF_4)_2$ ($C_{25}H_{22}B_2ClCuF_8N_5O_6S_2$)	Brown (90)	230	36.42 (36.36)	2.84 (2.67)	8.48 (8.48)	7.69 (7.76)	7.76 (7.69)	1.83	99
$[Zn(LOR)(Phen)(H_2O)_2](BF_4)_2$ ($C_{25}H_{22}B_2ClF_8N_5O_6S_2Zn$)	Brown (85)	250	36.49 (36.30)	2.74 (2.66)	8.68 (8.47)	7.85 (7.74)	7.86 (7.86)	Diam.	114

3.2. Molar conductance measurements

The molar conductance values of the synthetic complexes obtained in DMF as a solvent at room temperature are listed in Table 1. The results given in Table 1 showed that the Ni(II) complex has a molar conductivity value of 12, which indicated the non-ionic nature of this complex and hence its non-electrolytic nature [12].

The molar conductivity values of Mn(II), Fe(II), Co(II), Cu(II) and Zn(II) chelates under investigation (Table (1)) are found to be 130, 125, 145, 99 and 114 Ω^{-1} mol^{-1} cm^2, respectively. It is obvious from these data that these chelates are ionic in nature and they are of the type 1:2 electrolytes. Fe(III) complex have a molar conductance of 195 Ω^{-1} mol^{-1} cm^2 indicative that it is 1:3 electrolyte. In addition Cr(III) chelate has molar conductance of 80 Ω^{-1} mol^{-1} cm^2 indicative that it is 1:1 electrolyte [12, 13]

3.3. UV-visible studies

The UV–vis spectra of the free ligands and their metal (II) and (III) complexes are recorded in DMF solution in the wavelength range 200–700 nm (Fig. 2). The UV–vis spectrum of the free LOR ligand showed two absorption bands in the ultraviolet region at 294 and 373 nm. It follows from the literature that the bands at 294 and 289 nm for LOR and 1,10-phenanthroline, respectively, are related

to the π–π* transitions of the pyridine, thiophene and benzene rings [8-10]. The second absorption band in LOR drug at 373 nm may corresponds to the n–π* transition of the C= N and NH-CO groups.

In the metal complexes, the π–π* transition bands are shifted to 293–295 nm which can be attributed to the binding of these coordination centers to the central metal ions. The absorption band at 373 nm in free LOR ligand changes a bit in intensity and remains essentially slightly changed for Cr(III), Fe(II), Ni(II), Cu(II) and Zn(II) complexes, while this band disappear in Mn(II), Fe(III) and Co(II) ternary complexes [14, 15].

3.4. IR spectral studies

Infrared spectroscopy can be used as a good analytical tool to follow the complexation of the transition metal ions by the organic ligands [16, 17]. LOR as a bidendate natured ligand normally coordinates with metal ions through nitrogen of the pyridine ring and oxygen of the carbonyl group [18, 19]. The bands arising due to vibrational ν(C=N) mode at 1593 cm^{-1} and the ν(C=O) frequency in the free LOR drug at 1640 cm^{-1} were observed to be shifted to higher or lower frequencies, at 1510–1603 cm^{-1} and 1621–1657 cm^{-1}, respectively, in the metal complexes indicating the involvement of nitrogen of pyridine ring and oxygen of the amide group in the complex formation [18-20]. The two strong bands at 1330 cm^{-1} and 1037 cm^{-1} assigned to asymmetric and symmetric SO_2 vibration frequencies, respectively, in the free LOR ligand are remained intact in all complexes, indicating the non-participation of the SO_2 group in the chelation. Further, the complexes show a broad band in the range of 3389–3427 cm^{-1} which are the characteristics of ν(OH) [13, 20].

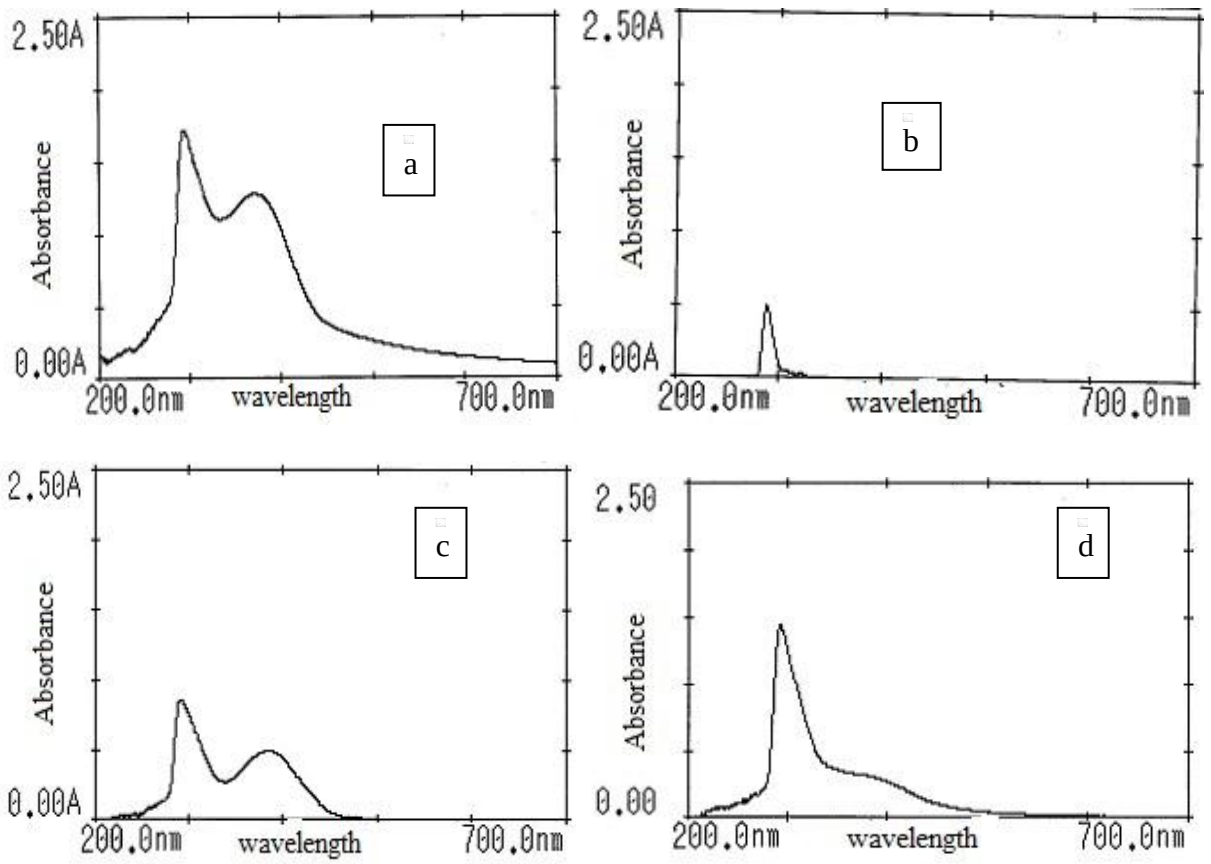

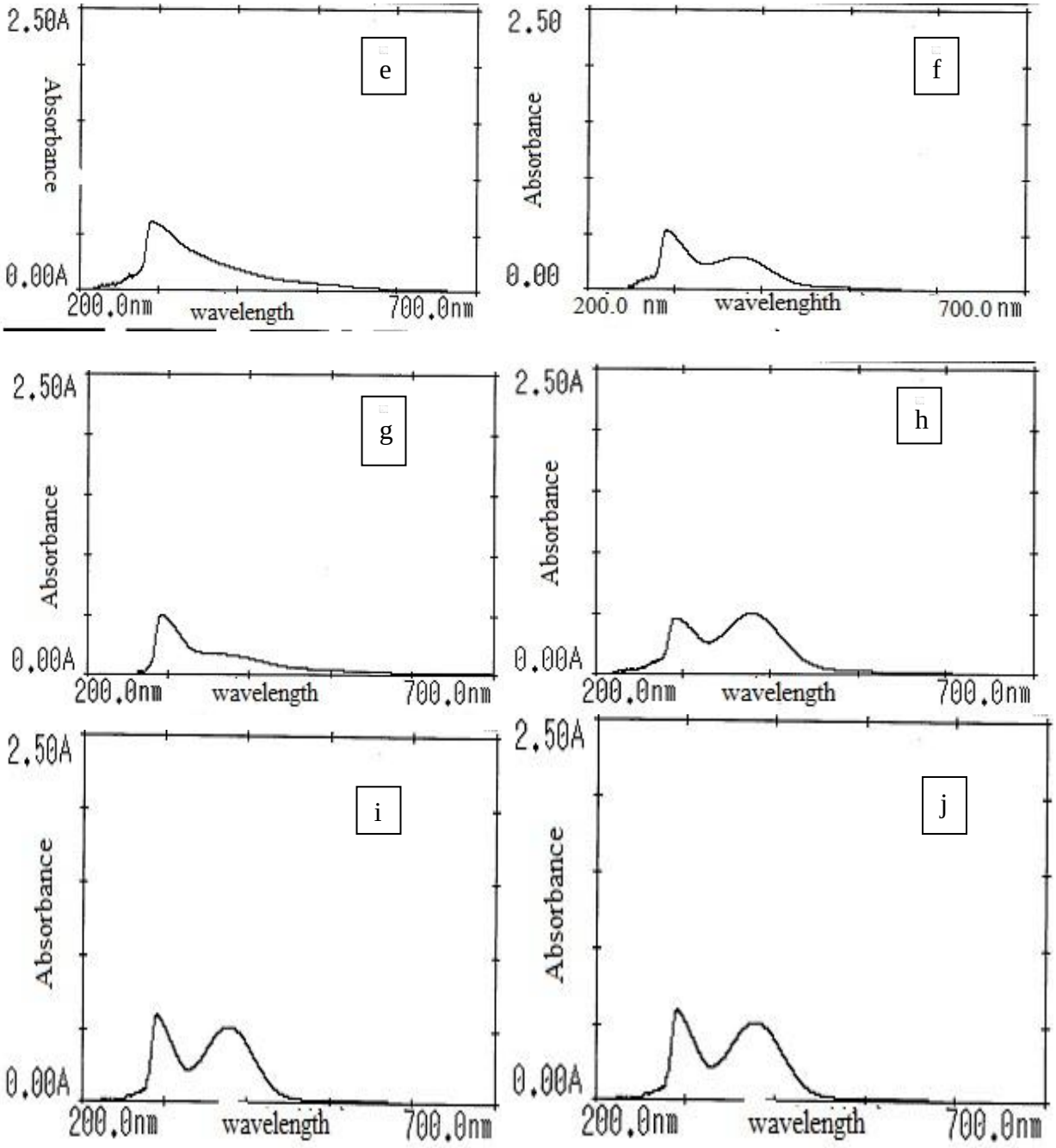

Figure 2. Uv-vis spectra of LOR ternary complexes with 1,10-phenanthroline (a) LOR , (b) 1,10-phenanthroline, (c) Cr(III), (d) Mn(II), (e) Fe(II), (f) Fe(III), (g) Co(II), (h) Ni(II), (i) Cu(II) and (j) Zn(II) complexes.

Strong band appearing at 1134 cm^{-1} is assigned to benzene and pyridine ring stretching vibrations in the free 1,10-phenanthroline. This band shows a slight shift to lower or higher wavenumber by 6–51 cm^{-1} (Table 2) indicating the coordination of the pyridine nitrogen atoms to the metal ions in a bidentate fashion [13, 20]. New bands found in the spectrum of the complexes lie in the range from 545 to 592 and 437 to 473 cm^{-1} that are not present in the spectrum of the ligand are attributed to ν(M-N) and ν(M-O) vibrations, respectively.

Table 2. IR spectra (4000-400 cm^{-1}) of LOR and its ternary metal complexes with 1,10-phenanthroline.

Lor	Phen	[Cr(LOR)(Phen)Cl_2]Cl.$2H_2O$	[$Mn(LOR)_2$(Phen)]$Cl_2.2H_2O$	[Fe(LOR)(Phen)$(H_2O)_2$]$(BF_4)_2$	[$Fe(LOR)_2$(Phen)]Cl_3	[Co(LOR)(Phen)$(H_2O)_2$]$(BF_4)_2$	[Ni(LOR)(Phen)Cl_2].H_2O	[Cu(LOR)(Phen)$(H_2O)_2$]$(BF_4)_2$	[Zn(LOR)(Phen)$(H_2O)_2$]$(BF_4)_2$	Assignment
3436br	-------	3418br	3396br	3411br	3422br	3416br	3389br	3427br	3427br	OH stretch
1640sh	------	1635s	1657s	1635s	1630s	1621s	1624s	1623s	1657s	CONH stretch
1593sh	1588s	1596s	1580s	1603s	1519s	1510s	1583s	1581s	1601s	C=N stretch
1330sh	-------	1344s	1337s	1348s	1331sh	1337s	1339s	1341s	1339s	SO_2 asym
--------	1134s	1153s	1150s	1145s	1152s	1151s	1157s	1140s	1086s	Benzene ring + pyridine ring stretch
1037s	-------	1042s	1047s	1045s	1031s	1049s	1049s	1056s	1043s	SO_2 sym
621s	--------	629s	630s	630s	630	629s	632s	615s	625s	C=N bend
---------	--------	571s	558s	563s	563s	588s	592s	553s	545s	M-O stretching
--------	--------	----------	----------	521s	----------	523s	----------	----------	514s	M-O stretch of coordinated water
--------	--------	459s	460s	463s	472s	466s	461s	437s	457s	M-N stretching
---------	--------	----------	----------	918s, 841s	----------	910s, 842s	----------	----------	920s, 853s	H_2O stretching of coordinated water

sh = sharp, m = medium, br = broad, s = small, w = weak

In addition, the bands of coordinated water were observed at 841-853 cm^{-1} and the υ(M-O) stretching vibrations of coordinated water attachment to metal ions are found at 521, 523 and 514 cm^{-1} for Fe(II), Co(II) and Zn(II) complexes, respectively, [19,21]. Furthermore, strong evidence for the presence or absence of coordinated water was supported by the thermal analysis studies of these complexes.

3.5. ^1H NMR spectral studies

Table 3. ^1H NMR spectral data of the lornoxicam drug and its ternary metal chelates with 1,10-phenanthroline.

Compound	Chemical shift, (δ) ppm	Assignment
LOR	9.90	(s, H,OH)
	7.20-7.90	(m, 5H, pyridine ring and thiophene CH)
[Zn(LOR)(Phen)$(H_2O)_2$]$(BF_4)_2$	9.95	(s, H,OH)
	7.01 – 7.95	(m, 13H, pyridine ring, thiophene CH of LOR, pyridine and aromatic rings of 1,10-phenanthroline)
	4.48	(s, H, NH)
	2.75	(s, 3H, N-CH_3)

The ^{1}H NMR spectra of a DMSO-d_6 solution of lornoxicam ligand (LOR) and its Zn(II) ternary complex with 1,10-phenanthroline showed well resolved signals as expected (Table 3). The spectrum of the free LOR showed singlet peak at 9.90 ppm (s, 1H) and multiplite signal at 7.20-7.90 ppm (m, 5H, pyridine ring and thiophene CH) which can be attributed to the OH group and aromatic pyridine and thiophene protons. The characteristic proton signals at 4.49 ppm (s, 1H) and 2.93 ppm (s, 3H) are assigned to NH and N-CH_3 groups, respectively.

The ^{1}H NMR spectrum of $[Zn(LOR)(Phen)(H_2O)_2](BF_4)_2$ complex (Table 3) showed the resonance with expected integrated intensities. The shift to higher field of pyridine and thiophene ring proton signal to 7.01 – 7.95 ppm (m, 13H) for Zn(II) ternary complex [22] which appears in the free LOR at 7.20-7.90 ppm, suggesting the coordination to the metal ions via the pyridyl nitrogen of both LOR and 1,10-phenanthroline. The signals observed at 3.33 ppm and 3.34 ppm with an integration corresponding to four protons in case of Zn(II) complex were assigned to two coordinate water molecules.

3.6. Mass spectra

The mass spectra of $[Co(LOR)(Phen)(H_2O)_2](BF_4)_2$ (Figure 3) and $[Ni(LOR)(Phen)Cl_2].H_2O$ (Figure 4) complexes showed peaks attributed to the molecular ions m/z at 819 and 698 M^+ for cobalt(II) and nickel(II) complexes, respectively. This data is in good agreement with the proposed molecular formula for these complexes. The parent LOR ligand peak appears in the mass spectra of both complexes at 371 amu confirming the complex formation. The mass spectral data support the structures of mononuclear transition metal complexes. The fragmentation pattern of the complexes does not show any loss of water or chlorine which is present outside the coordination sphere.

3.7. Magnetic moment measurements

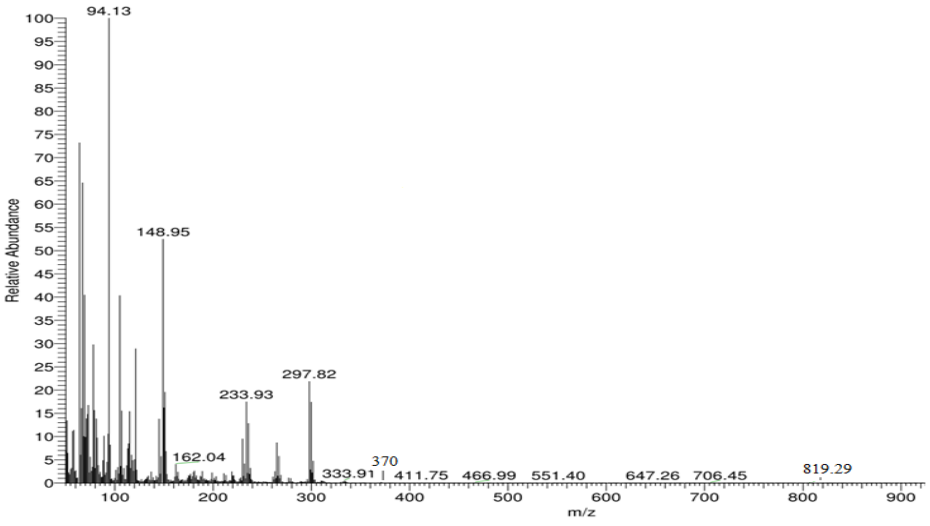

Figure 3. Mass spectra of $[Co(LOR)(Phen)(H_2O)_2](BF_4)_2$ complex.

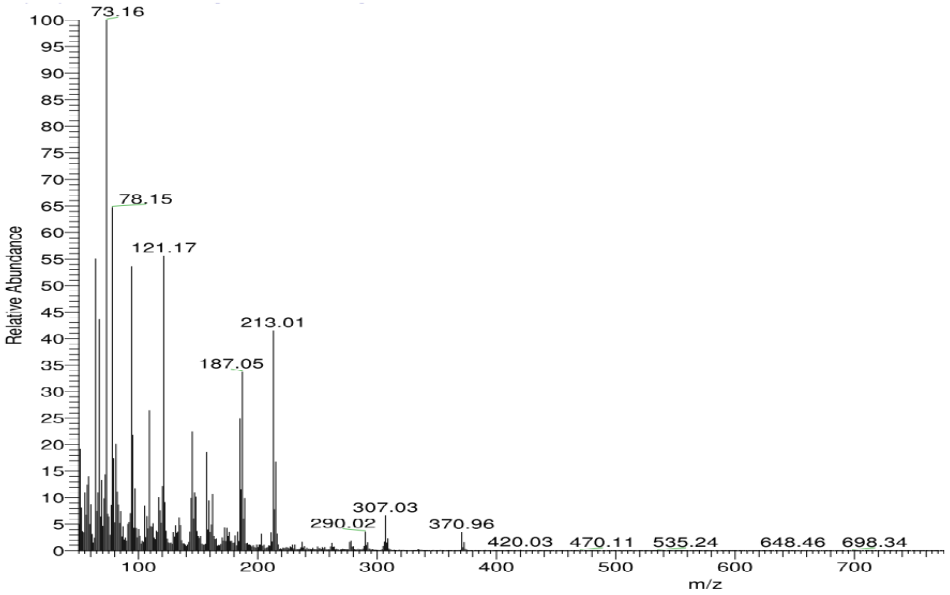

Figure 4. Mass spectra of [Ni(LOR)(Phen)Cl_2].H_2O complex.

The magnetic moment values are listed in Table 1. The magnetic moment values are found to be 4.87, 5.12, 5.33, 5.64, 5.20, 2.99 and 1.83 BM for Cr(III), Mn(II), Fe(II), Fe(III), Co(II), Ni(II) and Cu(II) complexes, respectively, suggesting an octahedral geometry [13, 22, 23]. The Zn(II) complex is diamagnetic and according to its empirical formula, an octahedral geometry was proposed for this complex.

3.8. Diffused reflectance spectral studies

A comparison of the electronic spectra of the free LOR drug and 1,10-phenanthroline ligands coordinated with those of the corresponding metal complexes, some shifts were detected. This can be considered as evidence for the complex formation. Additionally, the diffused reflectance spectra of metal complexes show different bands at different wavelengths, each one is corresponding to certain transition which suggests the geometry of the complexes. The diffused reflectance spectra of the complexes are dominated by intense intra-ligand charge transfer bands.

The diffused reflectance spectrum of Cr(III) complex exhibits three bands at 28,411, 26,459 and 13,452 cm^{-1} which may be assigned to the $^4A_{2g}(F)\rightarrow{}^4T_{2g}(F)$, $^4A_{2g}(F)\rightarrow{}^4T_{2g}(F)$ and $^4A_{2g}(F)\rightarrow{}^4T_{2g}(P)$ spin allowed d–d transitions, respectively, suggesting an octahedral geometry [13, 22-25].

The diffused reflectance spectrum of Mn(II) complex exhibits three bands at 26,418, 19,211 and 15,832 cm^{-1} which may be assigned to $^4T_{1g}\rightarrow{}^6A_{1g}$, $^4T_{2g}(G)\rightarrow{}^6A_{1g}$ and $^4T_{1g}(D)\rightarrow{}^6A_{1g}$ transitions, respectively, which suggests an octahedral geometry [13, 24, 25].

From the diffused reflectance spectrum, it is observed that, the electronic absorption spectra of Fe(II) and Fe(III) complexes show three weak bands at 20,040 and 19,940, 21,318 and 21,310 and

25,875 and 26,085 cm^{-1}, which may be assigned to the transitions $^6A_{1g}\rightarrow T_{2g}(G)$, $^6A_{1g}\rightarrow{}^5T_{1g}$ and charge transfer, respectively, suggested an octahedral geometry for these complexes [21-24].

The electronic spectrum of Co(II) complex generally showed three absorption bands in the region at 29,820, 17,380 and 13,751 cm^{-1}which assigned to $^4T_{1g}\rightarrow{}^4T_{2g}(F)$, $^4T_{1g}\rightarrow{}^4A_{2g}(F)$ and $^4T_{1g}\rightarrow{}^4T_g(P)$ transitions, showing an octahedral geometry [23, 24] around the Co(II) ion.

The electronic spectral data of Ni(II) complex showed d-d bands in the region 25,235, 15,875 and 21,210 cm^{-1}, respectively, to assigned the transitions $^3A_{2g}(F)\rightarrow{}^3T_{2g}(F)$, $^3A_{2g}(F)\rightarrow{}^3T_{1g}(F)$ and $^3A_{2g}(F)\rightarrow{}^3T_{1g}$, which are characteristic of Ni(II) in octahedral geometry .

The Cu(II) complex showed broad bands at 25,213 and 13,335 cm^{-1} which may be described to $^2B_{1g}\rightarrow{}^2B_{2g}$, $^2B_{1g}\rightarrow{}^2E_g$ and $^2B_{1g}\rightarrow{}^2A_{1g}$ transitions, and attributed to an octahedral geometry around the Cu(II) ion [13, 24]. Furthermore, it showed a broad and very strong band at 29,199 cm^{-1} which was assigned to a ligand-metal (LMCT) charge transfer excitation.

The Zn(II) complex is diamagnetic. According to the empirical formulae, an octahedral geometry was proposed for this chelate.

3.9. ESR spectral studies

The ESR spectrum of the Cu(II) complex was recorded in DMSO at 300 and 77 K (Fig. 5). The observed spectral parameters show $g_{\parallel}$ (2.165) > $g_{\perp}$ (2.098) > g_e (2.0023) which is the characteristic of an octahedral geometry [26] The observed value for the exchange interaction parameter for the Cu(II) complex (G = 1.684) suggests that the significant exchange coupling is present and the misalignment is appreciable. The observed value of α^2 (0.86) of the complex is less than unity, which indicates the covalent character [27]. The magnetic moment of the copper (II) complex is found to be 1.81 B.M. indicative of an unpaired electron. The orbital reduction factors $K_{\parallel}$ and $K_{\perp}$ estimated from the expression, $K_{\parallel} = (g_{\parallel} - 2.0023)\ \Delta E/8\lambda$, $K_{\perp} = (g_{\perp} - 2.0023)\ \Delta E/2\lambda$, λ=-828 cm^{-1} (spin – orbit coupling constant for the free ion). In case of a pure σ bonding $K_{\parallel} \cong K_{\perp} = 0.77$ whereas $K_{\parallel} < K_{\perp}$ implies considerable in-plane π -bonding while for out of π bonding $K_{\parallel} > K_{\perp}$. For this complex, $K_{\parallel} > K_{\perp}$ indicating poor in-plane π-bonding which is also reflected in β^2 value.

The ESR spectra of the solid Fe(III), Co(II) and Ni(II) complexes at room temperature do not show ESR signal because the rapid spin lattice relaxation of the Fe(III), Co(II) and Ni(II) (Fig. 5) complexes which broadness the lines at higher temperatures [28, 29]. The ESR spectra only show signals that may be accounted for the presence of free radicals that can resulted from the cleavage of any double bond and distribution of the charge on the two neighbor atoms.

3.10. X-ray powder diffraction

X-ray powder diffraction pattern in the $0^o < 2\theta < 60^o$ of the LOR and 1,10-phenanthroline ligands and their metal complexes were carried out in order to give an insight about the lattice dynamics of these complexes. The X-ray powder diffraction obtained reflects a shadow on the fact that

each solid represents a definite compound of a definite structure which is not contaminated with starting materials.

The XRD spectra for chelates show that the coordination of LOR and Phen ligands to the present metal ions [Cr(III), Mn(II), Fe(II), Fe(III), Co(II), Ni(II), Cu(II) and Zn(II)] changes the XRD pattern of the ligands. This means that the complexes are not fitted in the same phase of LOR and phen. In addition, on comparing the XRD spectra of the ternary chelates with the XRD spectra of the free ligands, it is concluded that all ternary chelates under study can be considered to have amorphous structures as they lack sharp peaks. The pattern for the Ni(II) complex is characteristic of crystalline phase.

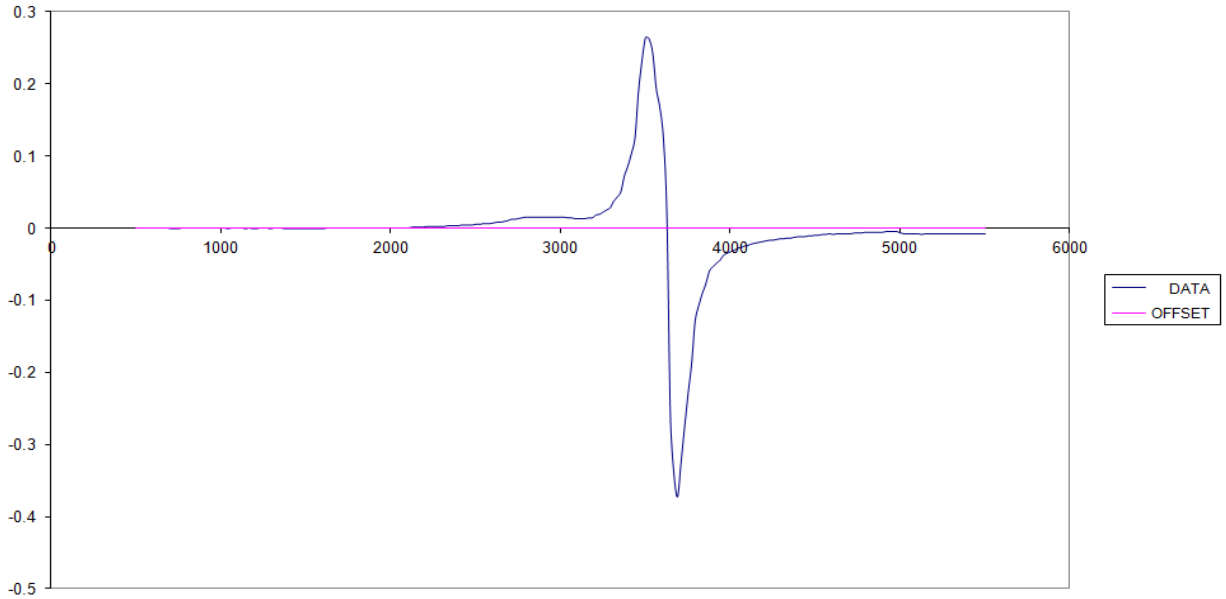

Figure 5. ESR spectra of $[Cu(LOR)(Phen)(H_2O)_2](BF_4)_2$ complex.

3.11. Thermal analysis studies

The decomposition stages, temperature ranges, percentage losses in mass and assignment of decomposition moieties are given in Table 4.

The thermal degradation of the 1,10-phenanthroline ligand occurred in two steps. The first stage is the loss C_2H_2 gas with mass losses of (obs. = 14.65%, calc. = 14.43%) within a temperature range of 30-120 °C. The next stage involves the loss of the organic fraction, $C_{10}H_6N_2$, within the temperature range of 120-320 °C, with mass losses of (obs. = 85.22%, calc. = 85.46%).

The Cr(III) complex decomposed in three stages. Stage one is between 30-140 °C, which indicates the loss of two molecules of water of hydration, with mass loss of (obs. = 4.46%, calc. = 4.82%). The second stage is within the temperature range of 140-370 °C, and is attributed to the loss of the organic moiety, $C_{18}H_{15}N_3Cl_2$, with mass losses of (obs. = 46.07%, calc. = 46.09%). The final stage is the loss of the organic moiety, $C_6H_3Cl_2N_2O_{2.5}S_2$, between 370-720 °C with mass losses of (obs. = 37.87%, calc. = 37.25%) leaving behind carbon and chromium oxide residues.

Table 4. Thermoanalytical results (TG and DTG) of LOR and its ternary metal complexes with 1,10-phenanthroline.

Complex	TG range (°C)	DTG_{max} (°C)	n*	Mass loss Estim (Calcd) %	Total mass loss	Assignment	residues
1,10-phenanthroline	30-120	99	1	14.65 (14.43)		- Loss of C_2H_2.	----------
	120-320	228	1	85.22 (85.46)	99.87 (99.89)	- Loss of $C_{10}H_6N_2$.	
$[Cr(LOR)(Phen)Cl_2]$ $Cl.2H_2O$	30-140	69	1	4.46 (4.82)		- Loss of $2H_2O$.	
	140-370	191	1	46.07 (46.09)		- Loss of $C_{18}H_{15}N_3Cl_2$.	C +
	370-720	520	1	37.87 (37.25)	88.40 (88.16)	- Loss of $C_6H_3Cl_2N_2O_{2.5}S_2$.	$½Cr_2O_3$
$[Mn(LOR)_2(Phen)]$ $.Cl_2.2H_2O$	30-150	56	1	3.29 (3.32)		- Loss of $2H_2O$.	
	150-390	198	1	45.60 (45.55)		- Loss of $C_{14}H_{18}Cl_3N_3O_4S_3$.	4C +
	390-760	467, 607	2	41.22 (41.22)	90.11 (90.09)	- Loss of $C_{20}H_{10}ClN_5O_3S$.	MnO
$[Fe(LOR)_2(Phen)]Cl_3$	30-310	228	1	40.93 (40.73)		- Loss of $C_{13}H_{10}Cl_3N_3O_4S_2$.	5C +
	310-580	393, 492	2	46.20 (46.31)	87.13 (87.04)	- Loss of $C_{20}H_{18}Cl_2N_5O_{2.5}S_2$.	$½Fe_2O_3$
[Fe(LOR)(Phen) $(H_2O)_2](BF_4)_2$	30-150	70	2	4.86 (4.89)		- Loss of 2HF.	B_2O_3 +
	150-350	200	1	51.47 (51.27)		- Loss of $C_{16}H_{10}ClF_4N_3S_2$.	$½Fe_2O_3$
	350-750	363,480, 623	3	25.56 (25.43)	81.89 (81.58)	- Loss of $C_9H_{10}F_2N_2O_{1.5}$.	
[Co(LOR)(Phen) $(H_2O)_2](BF_4)_2$	30-150	69	1	7.39 (7.56)		- Loss of $2H_2O$ and C_2H_2.	CoO +
	150-300	201	1	46.99 (46.77)		- Loss of $C_{13}H_{10}ClF_4N_3S_2$.	B_2O_3
	300-760	337, 613	2	30.93 (30.93)	85.31(85.29)	- Loss of $C_{10}H_6F_4N_2O_{1.5}$.	
$[Ni(LOR)(Phen)Cl_2]$ $.H_2O$	30-260	257	1	37.93 (37.91)		- Loss of H_2O and $C_{12}H_{11}N_2S_2$.	NiO
	260-700	400, 700	2	51.59 (51.43)	89.52 (89.34)	- Loss of $C_{13}H_7Cl_3N_3O_3$.	
[Cu(LOR)(Phen) $(H_2O)_2](BF_4)_2$	30-150	49	1	4.41 (4.36)		- Loss of $2H_2O$.	CuO +
	150-435	273, 379	2	26.07 (26.12)		- Loss of $C_{12}H_8ClN_2$.	B_2O_3
	435-780	588	1	51.01 (51.14)	81.49 (81.62)	- Loss of $C_{13}H_{10}F_8N_3S_2$.	
[Zn(LOR)(Phen) $(H_2O)_2](BF_4)_2$	30-140	35	1	4.14 (4.36)		- Loss of $2H_2O$.	ZnO +
	140-250	198	1	51.57 (51.60)		- Loss of $C_{17}H_{10}ClF_3N_4S_2$.	B_2O_3
	250-720	331,463, 582	3	25.92 (25.77)	81.63 (81.73)	- Loss of $C_8H_8F_5N$	

n* = number of decomposition step.

The decomposition of the Mn(II) complex occurs in four steps. The first step is within a temperature range of 30-150°C and corresponds to the loss of two moles of hydrated water with mass loss of (obs. = 3.29%, calc. = 3.32%). The successive decomposition occurs within a temperature range of 150-390 °C and equals the loss of the organic moiety, $C_{14}H_{18}Cl_3N_3O_4S_3$, with mass losses of (obs. = 45.60%, calc. = 45.55%). The final stage is the loss of the organic moiety, $C_{20}H_{10}ClN_5O_3S$, between 390-760 °C with mass losses of (obs. = 41.22%, calc. = 41.22%). The final product is carbon and manganese oxide residues with total mass loss amounts to (obs. = 90.11%, calc. = .90.09%).

The TG curve of the Fe(III) complex reveals three steps decomposition. The first step corresponds to the loss of $C_{13}H_{10}Cl_3N_3O_4S_2$ organic moiety with mass losses of (obs. = 40.93%, calc. = 40.73%) between 30-310 °C. The second and third steps are within the temperature range 310-580 °C, attributed to the loss of the organic moiety, $C_{20}H_{18}Cl_2N_5O_{2.5}S_2$, with mass losses of (obs. = 46.20%, calc. = 46.31%). The remaining fraction is ferric oxide and carbon residues.

The Fe(II) complex decomposes in six stages. The first two steps involves the loss of two moles of HF with mass losses of (obs. = 4.86%, calc. = 4.89%) between 30-150° C. The third stage is within the temperature range of 150-350 °C and corresponds to the loss of $C_{16}H_{10}ClF_4N_3S_2$, with mass loss of (obs. = 51.47%, calc. = 51.27%). The last three phases are within the temperature range from 350-750°C, and correspond to the loss of the organic moiety, $C_9H_{10}F_2N_2O_{1.5}$, with mass losses of (obs.

= 25.56%, calc. = 25.43%). The total weight loss amounts to (obs. = 81.89%, calc. = 81.58%) and the remaining fraction is boron and ferric oxides.

The Co(II) complex decomposes in four stages within the temperature range from 30-760 ◦C. The stage one is between 30-150 °C, which indicates the loss of two moles of water of hydration and one mole of C_2H_2, with mass losses of (obs. = 7.39%, calc. = 7.56%). The second stage is within the temperature range of 150-300 °C, which corresponds to the loss of the organic moiety, $C_{13}H_{10}ClF_4N_3S_2$, with mass losses of (obs. = 46.99 %, calc. = 46.77%). The final stages are between 300-760 °C and is attributed to the loss of the organic moiety, $C_{10}H_6F_4N_2O_{1.5}$, with mass losses of (obs. = 30.93%, calc. = 30.93%), leaving behind the cobalt and boron oxide residues.

The Ni(II) complex decomposes in three phases. The first phase is between 30-260 °C and is assigned to the loss of one water molecule of hydration and the organic fragment, $C_{12}H_{11}N_2S_2$, with mass loss of (obs. = 37.93%, calc. = 37.91%). The final phases are within the temperature range of 260-700 °C which corresponds to the loss of the organic moiety $C_{13}H_7Cl_3N_3O_3$, with mass losses of (obs. = 51.59%, calc. = 51.43%) leaving behind nickel oxide residue.

The thermogram of Cu(II) complex represents four stages of decomposition within the temperature range of 30-780 ◦C. The first stage at 30-150 ◦C with weight loss of (obs. = 4.41, calcd.= 4.36%) is corresponding to the loss of two coordinated water molecules. The second and third steps with weight loss of (obs. = 26.07, calc. = 26.12%) at 150-435 ◦C are attributed to the elimination of $C_{12}H_8ClN_2$ molecule. The fourth step at 435-780 ◦C with weight loss of (obs. = 51.01, calcd. = 51.14%) is referring to the removal of $C_{13}H_{10}F_8N_3S_2$ molecule. The residual part is CuO and B_2O_3.

The TG curve of Zn(II) complex shows five steps of decomposition. The first step corresponds to the elimination of two coordinated water molecules with weight loss of (obs. = 4.14%, calc. = 4.36%). This is followed by loss of $C_{17}H_{10}ClF_3N_4S_2$ fragment with weight loss of (obs. = 51.57%, calc. = 51.60%) in the temperature range of 140-250 ◦C. The third and fourth steps occurs within the temperature range of 250-720 ◦C and can be attributed to the loss of C8H8F5N organic molecule with mass loss of (obs. = 25.92%, calc. = 25.77%) leaving zinc and boron oxides as residues.

Thus, the decomposition patterns corroborate the proposed formulation of the complexes, and it suggests the use of these complexes as metal source in metal organic chemical vapour deposition.

3.12. The kinetic studies

There has been increasing interest in determining rate dependent parameters of solid-state non-isothermal decomposition reactions by analysis of TG curves. Several equations have been proposed to analyze a TG curves and obtain values for kinetic parameters. In the present investigation the general thermal behaviour of the 1,10-phenanthroline ligand and the complexes in terms of stability ranges, peak temperatures and values of kinetic parameters, are shown in Table 5. The kinetic parameters have been evaluated using the following methods and the results obtained by these methods are compared with one another. The following two methods are briefly discussed.

Table 5. Thermodynamic data of the thermal decomposition of LOR and its ternary metal complexes with 1,10-phenanthroline.

Complex	Decomp.Temp. (°C)	E* (kJmol^{-1})	A (s^{-1})	ΔS* (KJmol^{-1})	ΔH* (kJmol^{-1})	ΔG* (kJmol^{-1})
LOR	185-376 367-670	18.99 (17.85) 51.96 (50.50)	8.48×10^{3} (1.02×10^{4}) 3.34×10^{5} (3.40×10^{5})	-90.88 (-93.73) -86.73 (-88.83)	17.11 (15.24) 47.45 (46.99)	37.74 (36.21) 94.46 (92.18)
[Cr(LOR)(Phen)Cl_2] Cl.2H_2O	30-140 140-370 370-720	17.86 (18.29) 78.77 (76.47) 56.64 (55.30)	4.70×10^{4}(4.90×10^{4}) 3.88×10^{5} (3.70 $\times10^{5}$) 1.21×10^{3} (1.66 $\times10^{3}$)	-85.89 (-83.76) -77.46(-78.64) -130.3 (-131.6)	72.89 (75.59) 86.05 (84.77) 53.23 (52.20)	23.22 (26.38) 102.1 (100.7) 101.9 (100.8)
[Mn(LOR)$_2$(Phen)] .Cl_2.2H_2O	30-150 150-390 390-760	21.64 (4.11) 40.54 (40.65) 40.54 (39.27)	1.86×10^{4} (1.26 $\times10^{4}$) 5.13×10^{3} (6.12 $\times10^{5}$) 6.18×10^{4}(6.78×10^{4})	-88.63 (-85.50) -125.66 (-127.0) -81.54 (-80.01)	21.33 (19.60) 38.88 (39.01) 36.06 (38.80)	24.69 (22.76) 63.77 (65.01) 79.93 (77.93)
[Fe(LOR)$_2$(Phen)]Cl_3	30-310 310-580	75.72 (76.13) 153.7(158.3)	4.39×10^{7} (3.21×10^{7}) 2.42×10^{6} (1.76 $\times10^{6}$)	-29.36 (-30.36) -230.3 (-241.0)	75.13 (76.14) 150.93(151.2)	77.24 (76.29) 147.5 (146.6)
[Fe(LOR)(Phen) $(H_2O)_2$]$(BF_4)_2$	30-150 150-350 350-750	48.56 (50.53) 76.32 (74.75) 230.1(228.1)	9.85×10^{4} (8.40×10^{4}) 3.25×10^{3} (3.03×10^{3}) 3.70×10^{8} (3.31×10^{8})	-142.82 (-140.9) -120.8 (-118.2) -119.4 (-116.3)	47.43 (44.23) 73.47 (72.09) 225.3 (227.3)	66.86 (68.46) 112.0 (113.9) 156.7 (157.4)
[Co(LOR)(Phen) $(H_2O)_2$]$(BF_4)_2$	30-150 150-300 300-760	166.4 (166.0) 126.5 (126.6) 23.26 (22.65)	2.31×10^{4} (2.01 $\times10^{4}$) 4.24×10^{7} (3.24×10^{7}) 1.46×10^{3} (2.51 $\times10^{3}$)	-89.29 (-90.21) -76.38 (-76.58) -74.95 (-75.61)	28.21 (29.18) 140.6 (139.1) 118.8 (117.9)	20.77 (19.88) 124.77 (125.1) 61.92 (63.92)
[Ni(LOR)(Phen)Cl_2] .H_2O	30-260 260-700	43.75 (44.64) 82.40 (85.58)	6.12×10^{2} (5.20 $\times10^{2}$) 2.01×10^{2} (1.65×10^{2})	-138.9 (-135.9) -147.2 (-148.9)	43.31 (57.64) 78.51 (47.91)	50.67 (52.50) 147.4 (147.6)
[Cu(LOR)(Phen) $(H_2O)_2$]$(BF_4)_2$	30-150 150-435 435-780	48.89 (45.15) 51.96 (51.49) 15.92 (18.84)	1.59×10^{6} (3.22×10^{6}) 3.34×10^{5} (2.40×10^{5}) 2.36×10^{7} (2.91×10^{7})	-56.24 (-54.73) -86.72 (-88.83) -220.8 (-221.8)	101.7 (99.56) 47.45 (49.99) 21.85 (20.54)	39.32 (36.85) 94.45 (96.17) 44.70 (45.24)
[Zn(LOR)(Phen) $(H_2O)_2$]$(BF_4)_2$	30-140 140-250 250-720	45.26 (46.89) 74.84 (75.48) 37.15 (37.55)	2.92×10^{4} (2.54×10^{4}) 5.23×10^{3} (4.18×10^{3}) 4.17×10^{3} (2.96 $\times10^{3}$)	-85.52 (-83.15) -150.2 (-153.2) -234.2 (-233.3)	49.98 (50.39) 72.69 (74.94) 35.51 (34.17)	28.40 (30.70) 105.4 (103.6) 58.06 (59.08)

[#] The data between parenthesis are obtained using Horowitz-Metzger equation while the data without parenthesis are obtained using Coats-Redfern equation.

3.12.1.Coats-Redfern equation

The Coats-Redfern equation (1), which is a typical integral method, can be represented as [30]:

$$\int_0^{\alpha} \frac{d\alpha}{(1-\alpha)^n} = \frac{A}{\alpha}\int_{T_1}^{T_2} \exp\left(\frac{-E^*}{RT}\right)dt$$

For convenience of integration, the lower limit T1 is usually taken as zero. This equation on integration gives: For convenience of integration, the lower limit T1 is usually taken as zero. This equation on integration gives:

$$\ln[-\ln(1-\alpha)/T^2] = -E^*/RT + \ln[AR/\varphi E^*]$$

A plot of left-hand side (LHS) against 1/T was drawn, E* is the energy of activation in kJ mol-1 and calculated from the slope and A in (s^{-1}) from the intercept. The entropy of activation ΔS* in (J $K^{-1}mol^{-1}$) was calculated by using equation:

$$\Delta S^* = R \ln\left(\frac{Ah}{K_B T_s}\right)$$

Where K_B is the Boltzmann constant, h is the Plank's constant and Ts is the DTG peak temperature [31].

3.12.2.Horowitz-Metzger equation

The Horowitz-Metzger equation is an illustrative of the approximation methods. These authors derived the relation [32]:

$$\log\left[\frac{\{1-(1-\alpha)^{1-n}\}}{(1-n)}\right] = \frac{E^*\theta}{2.303RT_s^2} \quad \text{for } n \neq 1$$

When n=1, the LHS of equation 4 would be log[-log (1-α)]. For a first-order kinetic process the Horowitz-Metzger equation may be written in the form:

$$\log\left[\log\left(\frac{w_\alpha}{w_\gamma}\right)\right] = \frac{E^*\theta}{2.303RT_S^2} - \log 2.303$$

Where θ = T-Ts, wγ = wα –w, wα = mass loss at the completion of the reaction; w = mass loss up to time t. The plot of log[log(wα /wγ)] versus θ was drawn and found to be linear from the slope of which E* was calculated. The pre-exponential factor, A, was calculated from the equation:

$$\frac{E^*}{RT_S^2} = \frac{A}{[\varphi \exp(-E^*/RT_S)]}$$

The entropy of activation, ΔS*, enthalpy of activation, ΔH* and Gibbs free energy, ΔG*, were calculated using the following equations;

$\Delta H^* = E^* - RT$

$\Delta G^* = \Delta H^* - T\Delta S^*$

It is clear that the thermal decomposition process of the three complexes indicate that the complexes are thermally stable. The positive ΔH* values postulate an endothermic nature of the formed complexes. The greater negative values of ΔS* from -266.01 to -52.80 (J mol^{-1} K^{-1}) reveal that the complexes are more ordered with thermodynamic stability. The greater positive values of E* indicate that the processes involving in translational, rotational, vibrational states and a changes in

mechanical potential energy for complexes [33, 34]. The positive sign of ΔG* for the investigated complexes reveals that the free energy of the final residue is higher than that of the initial compound, and all the decomposition steps are non-spontaneous processes. Also, the values of the activation, ΔG increases significantly for the subsequent decomposition stages of a given complex. This is due to increasing the values of TΔS* significantly from one step to another which overrides the values of ΔH*.

3.13. Structural interpretation

From all of the above observations, the structure of all complexes may be interpreted with a similar distribution of like coordinating sites, which coordinated to M(II)/(III) ions and takes place via the pyridyl N and carbonyl O atom. The structure information from these complexes is in agreement with the data reported in this paper based on the elemental analysis, IR, ESR, mass, ^{1}H NMR and electronic spectra measurements. Consequently, the structures proposed are based on octahedral geometry. The proposed structural formulas of the above complexes are summarized as three types of coordination as follow:

a) In case of Fe(II), Co(II) and Zn(II) complexes.

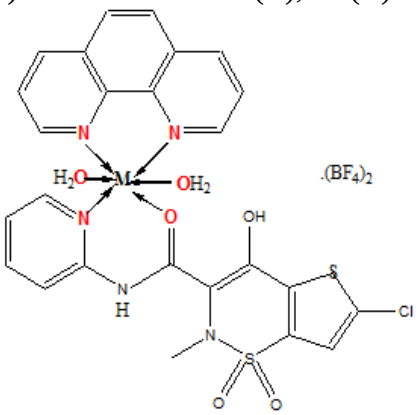

b) In case of Cr(III), Ni(II) and Cu(II) complexes (where n = 1, y = 2 for Cr(III) complex, n = 0, y = 1 for Ni(II) complex and n = 0, y = 2 for Cu(II) complex)

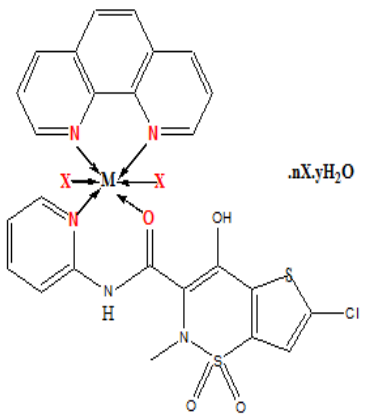

c) In case of Fe(III) and Mn(II) ternary complex (where n = 3, y = 0 for Fe(III) complex and n = 2, y = 2 for Mn(II) complex)

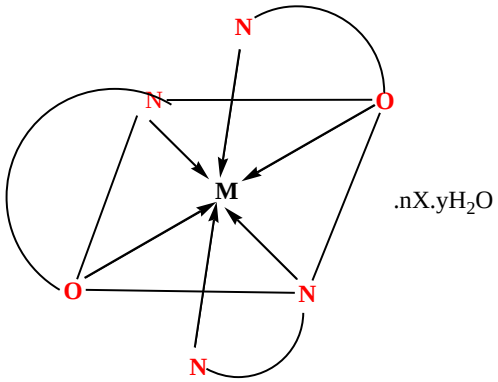

3.14. Antimicrobial activity

3.14.1. Antibacterial activities

Table 6. Biological activity of LOR ligand and its ternary metal complexes with 1,10-phenanthroline.

Sample	Inhibition zone diameter (mm / mg sample)				
	Bacillus subtilis	*Staphylococcus aureus*	*Neisseria gonorrhoeae*	*Escherichia coli*	*Candida albicans*
Control: DMSO	0	0	0	0	0
LOR	0	9	9	0	0
1,10-phenanthroline	38	28	36	43	35
$[Cr(LOR)(Phen)Cl_2]Cl.2H_2O$	13	12	10	12	0
$[Mn(LOR)_2(Phen)].Cl_2.2H_2O$	18	15	17	15	17
$[Fe(LOR)_2(Phen)]Cl_3$	10	10	12	11	0
$[Fe(LOR)(Phen)(H_2O)_2]. (BF_4)_2$	11	12	11	10	0
$[Co(LOR)(Phen)(H_2O)_2]. (BF_4)_2$	20	15	14	15	0
$[Ni(LOR)(Phen)Cl_2].H_2O$	0	0	0	0	0
$[Cu(LOR)(Phen)(H_2O)_2] (BF_4)_2$	11	13	11	12	0
$[Zn(LOR)(Phen)(H_2O)_2](BF_4)_2$	15	15	15	13	0
Amikacin	6	9	7	6	0
Ketokonazole	-	-	-	-	9

The antibacterial activities of the LOR and 1,10-phenanthroline ligands and ternary complexes against *Bacillus subtilis*, *Staphylococcus aureus*, *Beisseria gonorrhoeae* and *Escherichia coli* are presented in Table 6. The LOR ligand has no activity at all towards *Bacillus subtilis* and *Escherichia coli*. This is attributed to its very versatile nutritional capability, adaptability to various hydrocarbon rings, and the possession of pump mechanism which ejects metal complexes as soon as they enter the

cell [35]. In addition, *Bacillus subtilis, Staphylococcus aureus*, *Beisseria gonorrhoeae* and *Escherichia coli* are sensitive to all the complexes, with the exception of the Ni(II) complexes, and an inhibitory zone range of 10.0-20.0 mm (Fig. 6). In all cases, the metal complexes are more active than the LOR ligand expectedly due to chelation, which reduced the polarity of the metal atom, mainly because of partial sharing of its positive charge with donor groups of the ligand and possible π-electron delocalisation on the aromatic rings. This increased the lipophilic character, favouring its permeation into the bacterial membrane, causing the death of the organisms [36]. A look at the antibiotic, Amikacin, activities (6.0-9.0 mm) against the various bacterial isolates relative to the metal complexes (10.0-20.0 mm) showed that the activities of the former are much lower, with optimum activity being about half of metal complexes against all the bacterial organisms.

When the antimicrobial activity of metal complexes is investigated, the following principal factors [37] should be considered: (i) the chelate effect of the ligands; (ii) the nature of the N-donor ligands; (iii) the total charge of the complex; (iv) the existence and the nature of the ion neutralizing the ionic complex and (v) the nuclearity of the metal center in the complex. This is probably one of the reasons for the diverse antibacterial activity shown by the complexes while the nature of the metal ion coordinated to LOR ligand may have a significant role to this diversity. In general, all the complexes exhibit better inhibition than free LOR against *Bacillus subtilis*, *Staphylococcus aureus*, *Beisseria gonorrhoeae* and *Escherichia coli* (Table 6). More specifically, Mn(II) and Co(II) complexes show the best inhibition among all the complexes in this study and it is one and halt to twenty times more active than LOR against all the microorganisms used, indicating that the coordination of the LOR ligand to Co(II) and Mn(II) has enhanced its antimicrobial activity. On the other hand, the rest complexes present higher antimicrobial activity to LOR against the four microorganisms.

3.14.2. Antifungal activities

The preliminary fungitoxicity screening of the LOR, 1,10-phenanthroline and ternary complexes were performed against the *Candida albicans* in vitro by the diffusion technique [38]. LOR drug and all the metal complexes showed no fungal growth inhibition except Mn(II) complex. The Mn(II) complex in this study is nearly two times more active than Ketokonazole standard against *Candida albicans* microorganism used.

3.15. Anticancer activity

Cancer, of which there are over 100 different forms, is a leading cause of death. The clinical success of cis-platin, and related platinum based drugs, as anti-cancer agents constitutes the most impressive contribution to the use of metals in medicine [39]. However major problems associated with these anti-cancer metallo-drugs include serious toxicity and other side-effects, and major problems with resistance.

New potent and selective anti-cancer drugs are urgently required. Recently novel metal based compounds containing metals such as titanium, copper, ruthenium, tin and rhodium have been reported

with promising chemotherapeutic potential, and which have different mechanisms of vacation to the platinum based drugs [39-41].

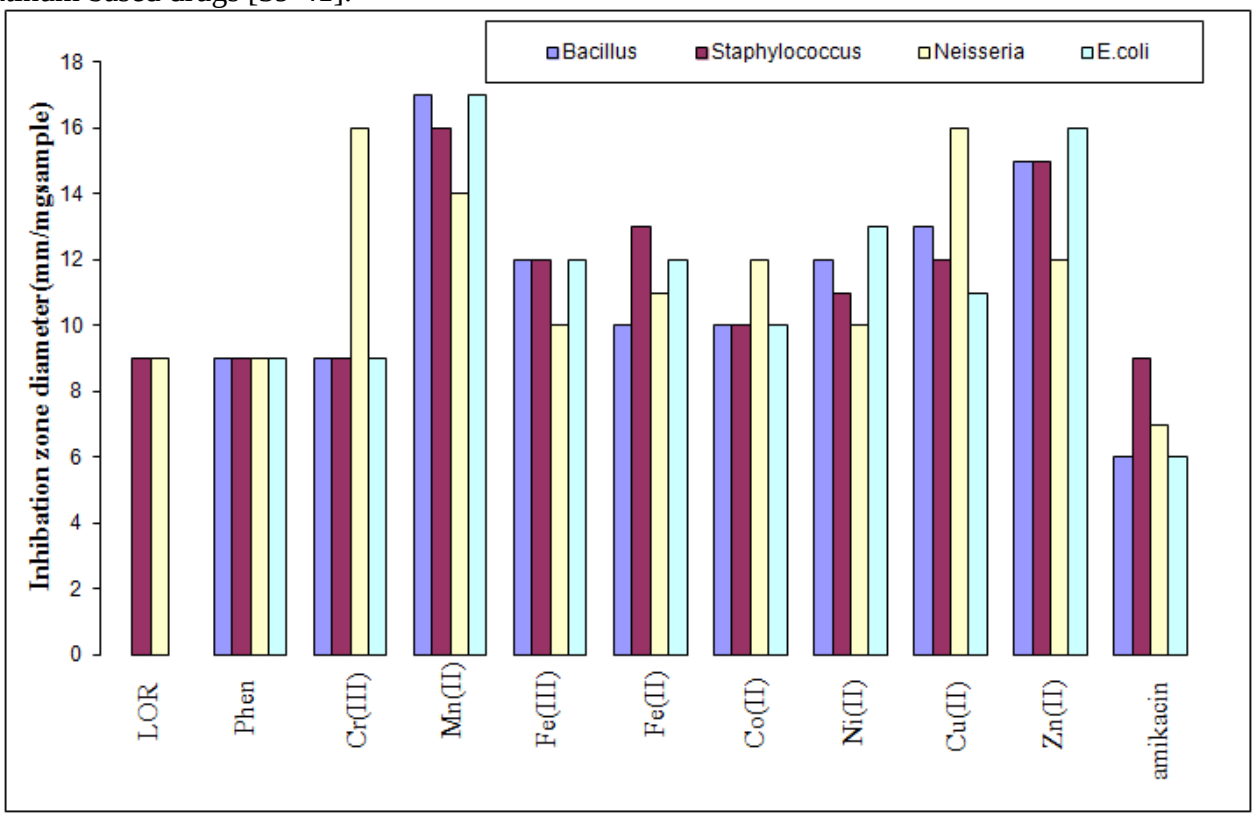

Figure 6. Biological activity of LOR, 1,10-phenanthroline and ternary complexes.

In previous studies, it has shown that the N,N-donor ligand 1,10-phenanthroline (Phen) and a range of its transition metal complexes are significantly more active (in vitro) anti-cancer agents than *cis*-platin against selected cancer cell lines [38]. Importantly, the Phen complexes are non-mutagenic (unlike *cis*- platin) and are not readily expelled from cells.

Table 7. Antibreastic cancer activity of LOR and its binary complexes.

Complex	Surviving fraction (MCF7)					IC_{50} (μg/ ml)
	Concn. (μg/ ml)	0.0	5	12.5	25	50
LOR		1.0	1.0	1.0	1.0	1.0	0.0
1,10-phenanthroline		1	0.482	0.318	0.315	0.297	4.73
$[Cr(LOR)(Phen).Cl_2]Cl.2H_2O$		1	0.757	0.508	0.428	0.345	13.7
$[Mn(LOR)_2(Phen)]Cl_2 \cdot 2H_2O$		1	0.522	0.508	0.353	0.351	12.7
$[Fe(LOR)_2(Phen).]Cl_3$		1	0.778	0.585	0.365	0.339	17.2
$[Fe(LOR)(Phen).2H_2O](BF_4)_2$		1	0.593	0.587	0.361	0.344	17.2
$[Ni(LOR)(Phen).Cl_2].H_2O$		1	0.857	0.748	0.604	0.519	23.1
$[Zn(LOR)(Phen)(H_2O)_2](BF_4)_2$		1	0.615	0.397	0.344	0.367	9

In this article, we demonstrated the inhibition activity of 1,10-phenanthroline and its ternary chelates with LOR against breast cancer derived cell lines (MCF7). It is obvious that Cr(III), Mn(II), Fe(II), Fe(III), Ni(II) and Zn(II) ternary complexes of LOR and Phen were found be very active against breast cancer cells with inhibition ratio values between 70% and 84%, while other complexes utilized in this work had been shown to be inactive (less than 70% inhibition). The IC_{50} values derived from the experimental data were summarized in Table 7.

It was interesting to note that 1,10-phenanthroline ligand showed higher inhibition activity and lower IC_{50} as compared to its metal complexes (Fig. 7).

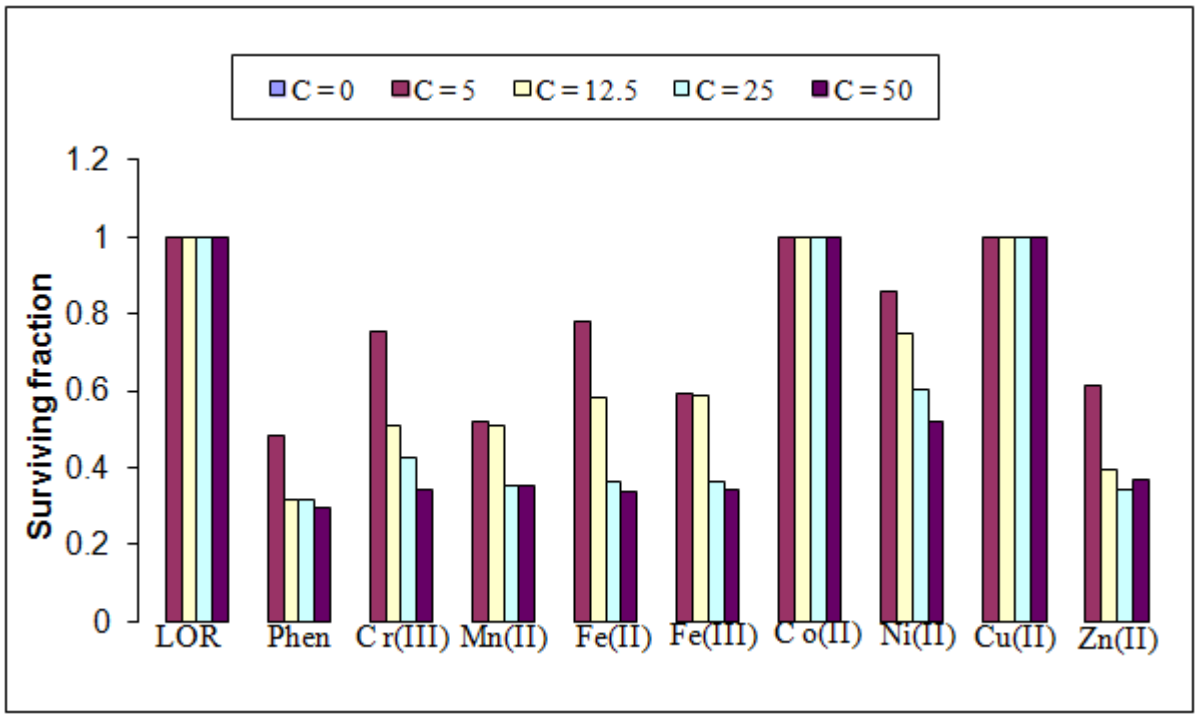

Figure 7. Anticancer activity of LOR, 1,10-phenanthroline and ternary complexes.

4. CONCLUSION

The work described in this paper involved the synthesis and spectroscopic characterization of a series of chromium, manganese, ferrous, ferric, cobalt, nickel, copper and zinc ternary complexes with LOR and 1,10-phenanthroline ligands. These complexes were characterized by using different physiochemical techniques. The IR spectra revealed that LOR behaves as neutral bidentate ligand coordinated to the metal ions through amide –CO and pyridine–N groups, also 1,10-phenanthroline behaves as neutral bidentate ligand coordinated to the metal ions through two pyridine–N groups. The magnetic moment and solid reflectance spectral measurements confirm the presence of all these chelates in octahedral geometry. The ESR spectra gave good evidence for the proposed structure and the bonding for all studied complexes. The antibreastic cancer test refers that 1,10-phenanthroline,

Cr(III), Mn(II), Fe(II), Fe(III), Ni(II) and Zn(II) ternary complexes recorded a significant inhibation efficiency against MCF7 cell line.

References

1. D. K. Demertzi, *J. Organomet. Chem.*, 691 (2006) 1767.
2. C. Bazzicalupi, A. Bianchi, C. Giorgi, B. Valtancoli, *Inorg. Chim. Acta*, 381 (2012) 229.
3. M.K. Motlagh, M. Noroozifar, A. Moodi, S. Niroomand. *J. Photochem. and Photobio. B:*
4. *Biology*, (2013), article in press.
5. M. Devereux, M. McCann, A. Kellett, *J. Inorg. Biochem.* 101 (2007) 881.
6. M.R.M. Hernandez, A. Mederos, S. Domínguez, A. Orlandini, C.A. Ghilardi, F. Cecconi, E.G. Vergara, A.R. Hernández, *J. Inorg. Biochem.*, 95 (2003) 131.
7. P.X. Franklin,A.D. Pillai,K.K. Vasu,V. Sudarsanam, *Eur. J. Med. Chem.*, 43 (2008) 129.
8. N. Vukovic, S. Sukdolak, S. Solujic, T. Milosevic, *Arch. Pharm.*, 341 (2008) 491.
9. S. Rover, M.A. Cesura, P. Huguenin, A. Szente, *J. Med. Chem.*, 40, 4378 (1997).
10. A.M. Panico, A. Geronikaki, R. Mgonzo, V. Cardile, B. Gentile, I. Doytchinova, *Bioorg. Med. Chem.*, 11 (2003) 2983.
11. I. Sakiyan, E. Logoglu, S. Arslan, N. Sari, *Biometals*, **17** (2004) 115.
12. P. Skehan, R. Storeng. *J. Natl. Cancer Inst.* 42 (1990) 1107.
13. W.M.I. Hassan, M.A. Badawy, G.G. Mohamed, H. Moustafa, S. Elramly. *Spectrochim. Acta A* , 111 (2013) 169.
14. G.G. Mohamed, H.F. Abd El-Halim, M.M.I. El-Dessouky, W.H. Mahmoud. *J. Mol. Str.*, 111 (2011) 29.
15. Y.T Liu, G.D. Lian, D.W. Yin, B.J. Su. *Spectrochim. Acta A*, 100 (2013) 131.
16. [S. Yadav, R.V. Singh. *Spectrochim. Acta A*, 78 (2011) 198.
17. L. Guo, S. Wu, F. Zeng, J. Zhao. *Eur. Polym. J.*, 42 (2006) 1670.
18. E. Rentschler, C. von Malotki, *Inorg. Chimica. Acta*, 361 (2008) 3646.
19. C.S. Dilip, V. S. Kumar, S.J. Venison, I.V. potheher, D. R.Subahashini. *J. Mol. Str.*, 1040 (2013) 192.
20. M.A. El-Ghamry, A.A. Saleh, S.M.E. Khalil, A.A. Mohammed. *Spectrochim. Acta A*, 110 (2013) 205.
21. M. Shebl, H.S. Seleem, B.A. El-Shetary. *Spectrochim. Acta Part A*, 75 (2010) 428**.**
22. T.A. Yousef, G.M. Abu El-Reash, O.A. El-Gammal, R.A. Bedier. *J. Mol. Str.*, 1035 (2013) 307.
23. A.M.A. Alaghaz, H.A. Bayoumi, Y. A. Ammar, S. A. Aldhlmani, *J. Mol. Str.*, 1035 (2013) 383.
24. F.A. Cotton, G. Wilkinson, C.A. Murillo, M. Bochmann, Advanced Inorganic Chemistry, sixth ed., Wiley, New York, 1999.
25. M. Hanif, Z.H. Chohan, *Spectrochim. Acta A*, 104 (2013) 468.
26. C.G. Richthofen, A. Stammler,H. Bogge,T. Glaser. *Eur. J. Inorg. Chem.* 36 (2012) 5934.
27. R.N. Patel, A. Singh, K.K. Shukla, D.K. Patel, V.P. Sondhiya, S. Dwivedi, *J. Sulfur Chem.*, 31 (2010) 299.
28. S.M. Annigeri, A.D. Naik, U.B. Gangadharmath, V.K. Revankar, *Transition Met. Chem.*, 27 (2002) 136.
29. M.F.R. Fouda, M.M. Abd-el-Zaher, M.M.E. Shadofa, F.A. El Saied, M.I. Ayad, A.S. El Tabl, *Trans. Met. Chem.*, 33 (2008) 219.
30. S. M. Abdallah, G. G. Mohamed, M.A. Zayed, M.S. Abou El-Ela. *Spectrochim. Acta A*, 73 (2009) 833.
31. A.W. Coats, J.P Redfern., *Nature*, 201 (1964) 68.
32. M. K. M.Nairand, P. K. Radhakrishnan, *Thermochim. Acta*, 261 (1995) 141.
33. H.W.Horowitz, G.Metzger. *Anal. Chem.*, 35 (1963) 1464.
34. P .Kofstad, *Nature*, 179 (1957) 1362.

35. A.A. Frost, R.G. Pearson, Kinetics and Mechanism-A Study of homogenous chemical reaction, Wiley, New York, 1961.
36. M.J. Pelczar, E.C.S. Chan, N.R. Krieg, "Host-Parasite Interaction; Nonspecific Host Resistance", In: Microbiology Concepts and Applications, 6th ed., McGraw-Hill Inc., New York, U.S.A., 1999, 478-479.
37. T.D. Thangadurai, K. Natarajan. *Int. J. Chem A*, 40 (2001) 573.
38. E.K. Efthimiadou, A. Karaliota, G. Psomas. *Polyhedron*, 27 (2008) 1729.
39. (a) N. Fahmi, M.K. Biyala, R.V. Singh. *Trans. Met. Chem.* 29 (2004) 681. (b) A. Hooda, V.K. Garg, N.K. Sangwan, K.S. Dhindsa. *Proc. Natl. Acad. Sci.* 66 (1996) 223.
40. H.F. Abd El-Halim, G.G. Mohamed, M.M.I. El-Dessouky, W.H. Mahmoud. *Spectrochim. Acta A*, 82 (2011) 8.
41. G. Tamasi, *The Open Crystallogr. J.*, 3 (2010) 41.
42. M. Maschke, M. Lieb, N.M. Nolte. *Eur. J. Inorg. Chem.* 36 (2012) 5953.